Indian Geotechnical Journal, 22 (2), 1992

Elastic Deformations of Reinforced Soil under Triaxial Stress Conditions

by

Madhira R. Madhav*

Introduction

The use of reinforced earth as a civil engineering material has gained widespread application all over the world. Thus earthwalls, embankments, abutments, etc., are routinely being constructed with this material. Reinforcement of ground for slopes, foundation beds, pavements, etc., is another application of the reinforcement principle. While the applications of reinforced earth and earth reinforcement have been extensive and varied, the design procedures are still empirical or semi-empirical due to inadequate understanding of the behaviour of reinforced earth.

The reinforcing elements vary from almost inextensible steel or G.I. strips, through moderately stiff geogrids to highly extensible geotextiles. The improvement in the over all behaviour of the composite is achieved through the interaction between the soil and the reinforcement. Due to the differences in their moduli of deformation of stiffnesses, shear stresses are mobilised at the interfaces between the soil and the reinforcement. The effect of the shear stresses is to generate tensile stresses in the reinforcement and to restrain the soil within, through these boundary shear stresses.

The restraint offered to the soil by the reinforcement, is quantified in terms of strength by the confining stress concept (Yang, 1972) or by the cohesion concept (Schlosser and Long, 1974). McGown *et al* (1978) investigate the effect of inclusion properties on the behaviour of sand based on plane strain tests. They distinguish between reinforced soil and plysoil based on the stiffness of the inclusions. Gray and Ohashi (1983) present results of direct shear tests conducted on sand reinforced with fibres of natural and synthetic materials. Ingold and Miller (1982) present a theory for predicting the undrained strength of a reinforced clay in plane strain conditions. An analysis for strength of reinforced granular soil under

*Professor, Deptt. of Civil Engg., Indian Institute of Technology, Kanpur, 208016, India

(The modified manuscript of this paper was accepted in Dec., 1991 *and is open for discussion till the end of December* 1992).

triaxial stress conditions is presented by Broms (1987, 1988). Most studies on reinforced soil thus pertain to the strength aspect alone.

Balla (1960) presented a general solution for the elastic stresses under triaxial compression, using the stress function approach to solve the biharmonic equation. Numerical results have been presented by him for the normal (axial, radial, and tangential) and shear stresses for a specimen with a height to diameter ratio of 2.0. This solution is analysed in the following section for axial and radial displacements of a reinforced soil under axisymmetric stress and strain conditions.

Analysis

A cylindrical soil specimen of diameter, d, and height, h, reinforced with rough rigid reinforcement discs spaced at a distance, S, is considered (Fig. 1*a*). The specimen is subjected to radial, (σ_3) and axial (σ_1) stresses. The soil contained between the two reinforcement layers at a spacing, S, is shown in Fig. 1(*b*). Balla (1960) presented a solution for stresses and displacements in a cylindrical specimen of radius, R and half height H (Fig. 1*b*) subjected to triaxial stress conditions but with rough ends. If the spacing between the reinforcement layers is S, the soil bounded by two reinforcement layers can be analysed based on Balla's solution with $H = S/2$ and

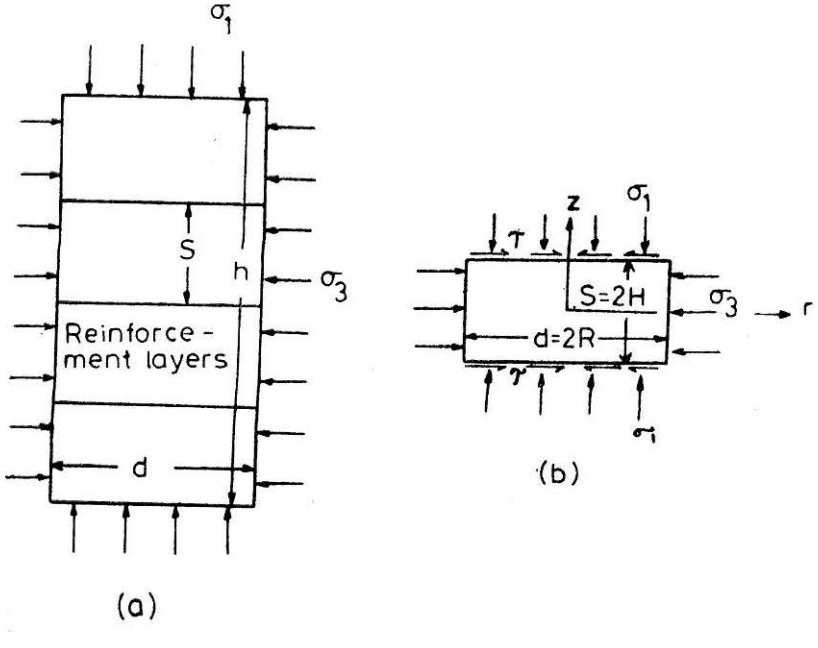

FIGURE 1 Definition Sketch (a) Reinforced soil Specimen (b Soil within two Reinforcement Layers

$R = d/2$. The vertical, w_s (r,z) and the radial, u_s (r,z) displacement of a point within the soil can be expressed as

$$w_s(r,z) = \frac{H}{E_s} \; I_1 \, \sigma_1 + I_2 \, \sigma_3 \tag{1}$$

$$u_s(r,z) = \frac{R}{E_s} \; I_3 \, \sigma_1 + I_4 \, \sigma_3 \tag{2}$$

where $H = S/2$, $R = d/2$, E_s–modulus of deformation of soil, and I_1 to I_4 are given in Appendix I. Coefficients I_1 to I_4 are functions of the ratios r/R, z/H,ν–the Poisson's ratio of the soil, and the parameter, Ψ, where

$$\Psi = 1 - \frac{u_{HR}}{u_{HR\ max}} \tag{3}$$

which is a measure of the frictional resistance between the soil and the reinforcement discs, u_{HR} and $u_{HR\ max}$—the radial displacements with and without friction, respectively of the edge of the soil specimen, $\Psi = 0$ implies a smooth reinforcement while $\Psi = 1$ corresponds to a fully restrained (laterally) specimen.

Eqs. (1) and (2) are rewritten as

$$w_s = H/E_s . \; \sigma_1 . \; I_w \tag{4}$$

$$u_s = \frac{R}{E_s} \; \sigma_1 \, I_r \tag{5}$$

where $I_w = I_1 + I_2 \, \sigma_3/\sigma_1$ and $I_r = I_3 + I_4 . \; \sigma_3/\sigma_1$

The total axial displacement of the soil contained between the two reinforcement layers is twice w_s (r,H) while the total axial compression of the triaxial specimen of height, h, is

$$w_h = 2 \; w_s \, (r,H) . \quad h/s \tag{6}$$

The restraining affect of the reinforcement is often expressed as an additional or equivalent confining stress. The vertical displacement of the soil bounded by two reinforcing discs can also be expressed in terms of the additional confining stress, $\Delta\sigma_3$, as

$$w_s = \frac{H}{E_s} \; [\sigma_1 - 2\nu_s \, (\sigma_3 + \nabla\sigma_3)] \tag{7}$$

or,

$$= H/E_s \; \sigma_1 \left\{ 1 - 2\nu_s \left(\frac{\sigma_3}{\sigma_1} + \frac{\Delta\sigma_3}{\sigma_1} \right) \right\} \tag{8}$$

Equating ws from Eqs. (3) and (7), the equivalent confining stress $\Delta\sigma_3$ is

obtained as

$$\frac{\Delta\sigma_3}{\sigma_1} = \frac{(1 - I_w)}{2\nu_s} - \frac{\sigma_3}{\sigma_1} \tag{9}$$

Alternatively an equivalent modulus of deformation, E_R, for the reinforced soil can be computed. The displacement, w_s, can also be expressed as

$$w_s = \frac{H}{E_R}\{\sigma_1 - 2\nu_s\,\sigma_3\} = \frac{H}{E_R}\,\sigma_1\{1 - 2\nu_s\,\sigma_3/\sigma_1\} \tag{10}$$

From Eq. (3) and (9), E_R is obtained as

$$E_R = E_s(1 - 2\nu_s\,\sigma_3/\sigma_1)/I_w \tag{11}$$

The equivalent additional confining stress, $\Delta\sigma_3$, and the ratio E_R/E_s are functions of the ratios S/d, σ_3/σ_1, Ψ, and ν_s. If spacing, S, between reinforcement layers equals, h, the results for a standard triaxial specimen with rough ends are obtained.

Results and Discussion

Balla (1960) presented the values of normal and shear stresses within a triaxial sample with s/d or h/d, $\nu_s = 1/3$, and $\Psi = 1.0$ (the radial movement of edge point *i.e.* $z = H$, $r = R$ is zero). Herein are given the computed values of axial and radial deformation for the following ranges of the parameters:

S/d : 0.01–2.0

ν_s : 0.2–0.5

Ψ : 0–1.0

σ_3/σ_1 : 0–1.0

Different values of S/d correspond to different spacings of reinforcement layers.

The variation of influence coefficient, I_w, with spacing ratio, S/d, is depicted in Fig. 2 for different confining stresses and for $\Psi = 1.0$ (full mobilization of friction on the top and bottom faces due to interaction with reinforcement). The reduction in the coefficient, I_w, with increasing number of reinforcing layers (decreasing values of S/d) is maximum for the unconfined specimen ($\sigma_3 = 0$).

For a specimen with S/d (or h/d) (the standard triaxial specimen) the coefficient, I_w, reduces from 1.0 for frictionless ($\Psi = 0$) to 0.925 for rough surfaces ($\Psi = 1.0$). The coefficient reduces to 0.85, 0.69, 0.54 and 0.45

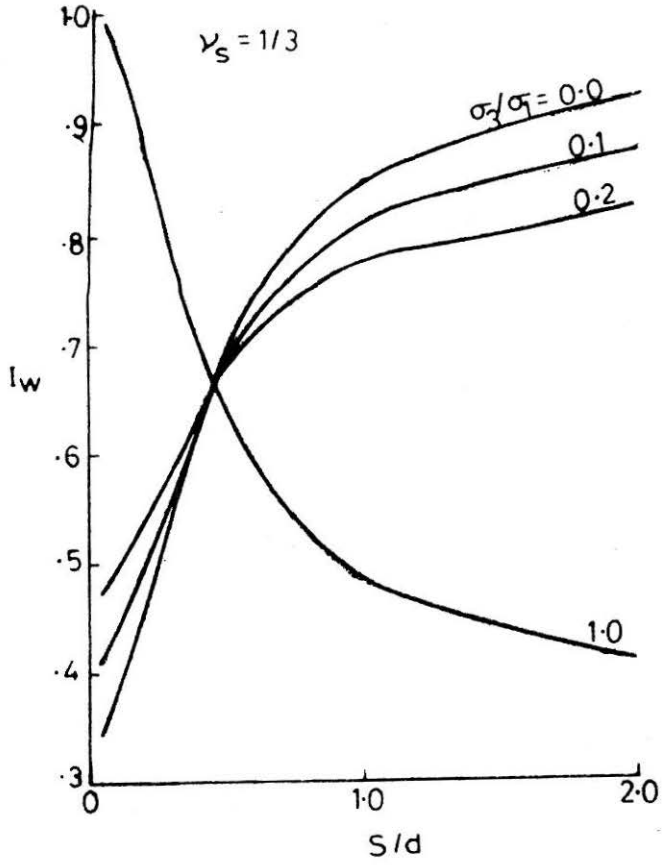

FIGURE 2 Displacement Coefficient I_w Versus Spacing—Effect of Confining Stress

for S/d values of 1.0, 0.5, 0.2 and 0.1 respectively. Thus the frictional forces mobilised by reinforcement significantly reduce the settlement of soil confined between the layers. This result is a consequence of the restraining effect on the radial (lateral) displacements on the end surfaces of the sample. Smaller the distance between the reinforcement layers, larger is the reduction in strains and deformations of the soil. Reinforcement provides restraint only if sufficient lateral displacements are likely to be mobilized. The radial expansion of a cylindrical specimen decreases with increasing confining pressure on it. Consequently, under high confining pressures, the restraining effect of the reinforcement is very less because the lateral deformations are small. I_w decreases with increasing values of σ_3 for S/d ratios greater than about 0.45. For S/d less than 0.45, the I_w values increase with confining stress. It is interesting to note that for $S/d = 0.5$, the coefficient I_w, is nearly constant and independent of the ratio σ_3/σ_1. With further increase in confining stress, the strain coefficients

exhibit a reversal in their trend, *i.e.* they decrease with increasing S/d values.

The Poisson's ratio, ν_s, of the soil, has significant effect on the coefficient, I_w (Fig. 3). For the unconfined sample with $S/d = 0.2$ and $\Psi = 1.0$, I_w decreases from 0.875 for $\nu_s = 0.2$ to 0 for $\nu = 0.4$. For the undrained condition, $\nu_s = .5$, the coefficient I_w becomes negative implying heave of the soil. Such apparently anamolous behaviour of heave under applied

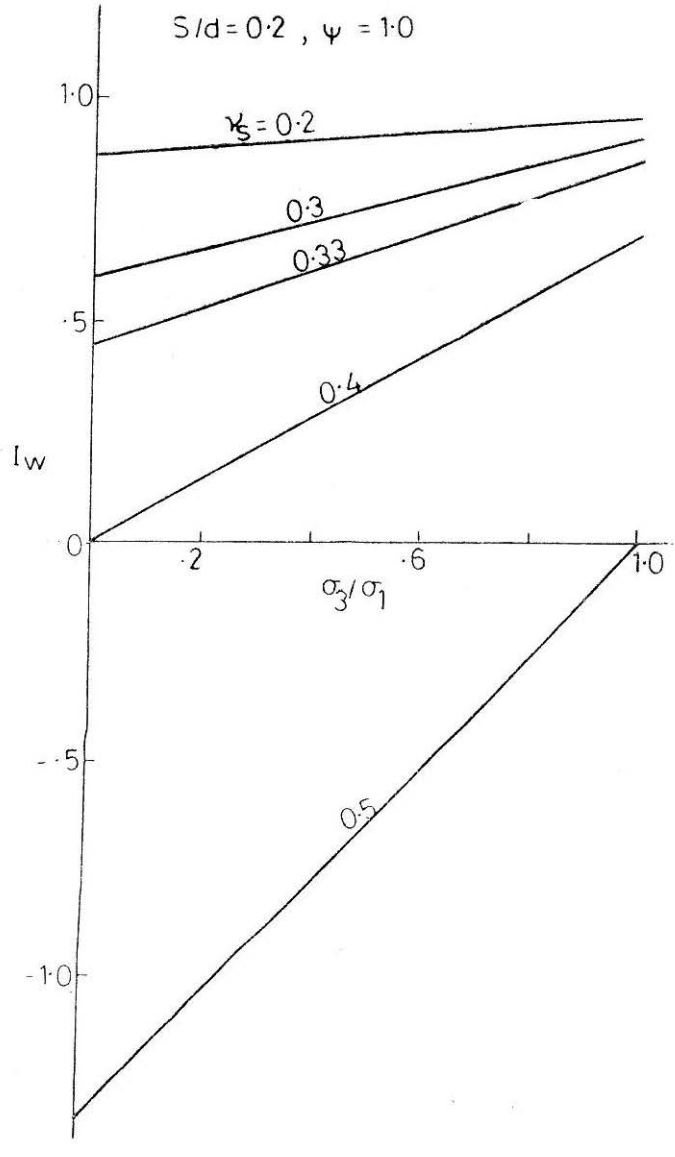

FIGURE 3 Displacement Coefficient I_w Versus Spacing—Effect of Poisson's Ratio

axial stress can be explained by the fact that if $\nu_s = 0.5$, the soil is incompressible (*i.e.* no volume change) and radial strains are equal to half the axial strain. If the lateral strains are large, the restraining shear stresses also are very high. The consequent equivalent confining stress due to the shear stresses mobilised are significantly large and enough to cause heave as in an extension test, specifically if the sample thickness is relatively small compared to its diameter. The coefficient I_w increases with confining stress since S/d is less than 0.45. It is noted that I_w is equal to zero (axial strain is zero) for the conditions (*i*) $\nu_s = 0.4$ and $\sigma_3 = 0$ and (*ii*) $\nu_s = 0.5$ and $\sigma_3 = \sigma_1$.

The displacement profiles for samples with $\nu = 0.3$, $\sigma_3 = 0$, $\Psi = 1.0$ and H/R equal to 2.0, 1.0 and 0.5 are shown in Fig. 4. For simplicity only one quarter of the sample is depicted. The arrows indicate the displacements undergone by the point after loading. For each point, the axial and radial displacements are marked and the initial and final position joined by an arrow. The scales for displacement coefficients I_r and I_w, are given in the figure. The top surface undergoes uniform axial displacement due to the imposed boundary condition (rigid end plates). Since $\Psi = 1.0$, the corner point is prevented from radial displacement. The radial displacements increase towards the centre of the sample. For $S/d = 2.0$, the tendency for more uniform displacements can be noted since the sample is relatively long and because of the St. Venant principle. The deformation conditions become highly nouniform for smaller values of

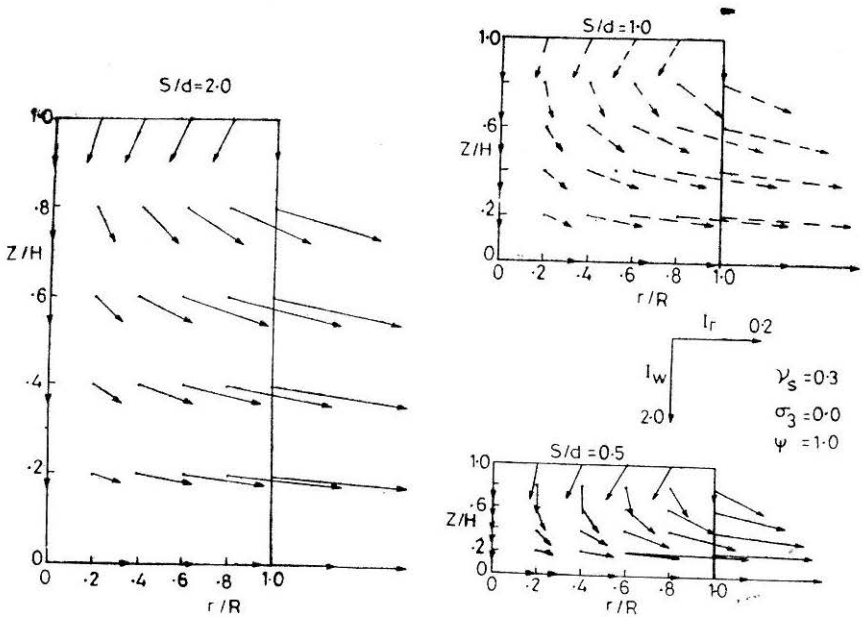

FIGURE 4 Displacement Profiles for S/d = 2.0, 1.0, and 0.5

S/d ratio due to the mobilized frictional stresses on the end of the sample because of reinforcement.

The effect of Poisson's ratio on displacement profile for sample with $S/d = 0.2$, $\sigma_3 = 0$ and $\Psi = 1.0$, is shown in Fig. 5. For $\nu_s = .2$, the points with $r/R \leqslant 0.8$ move inward while points near the outer periphery move outward for $z/H < 0.8$. The radial displacements increase from zero at the corner point to a maximum at the centre. The radial displacement on periphery of the sample increase with increasing values of Poisson's ratio. The reduction in axial displacements with ν explained earlier is once again noticeable.

The equivalent modulus of deformation, E_R, is computed based on Eq. 10 and depicted in Fig. 6 as a function of the spacing to diameter ratio, S/d. As can be expected, the modulus due to the elastic effects of restraining shear stresses, increases as the reinforcing layers get closer. For full mobilisation of friction ($\Psi = 1.0$), the modular ratio is 1.06, 1.12, 1.18 and 1.65 for S/d ratios of 2.0, 1.0, 0.5 and 0.2 respectively. For low values of S/d, the modular ratio is significantly larger.

The equivalent confining stress concept is another convenient way in which the effect of boundary shear stresses can be quantified. The equivalent confining stress, $\Delta\sigma_3$, is calculated from Eq. 8 and presented in Fig. 7. The trend in the variation of $\Delta\sigma_3/\sigma_1$ with S/d is very similar to that of E_R/E_s with S/d. The equivalent confining stress, $\Delta\sigma_3$, is 0.09, 0.18, 0.37 and 0.65 times σ_1 for S/d values of 2.0, 1.0, 0.5 and 0.2 respectively. This equivalent confining stress improves the stiffness of the soil further, according to the relation

$$E_o(\sigma_3) = E_{so}\,(\sigma_3/\sigma_{30})^n \tag{12}$$

where E_{so} is the modulus of deformation corresponding to a confining stress of σ_{30}, and n–a parameter.

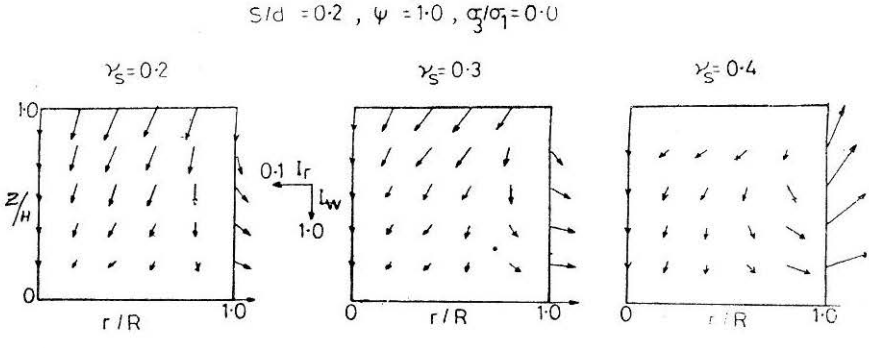

FIGURE 5 Displacement Profiles for S/d = 0.2—Effect of Poisson's Ratio

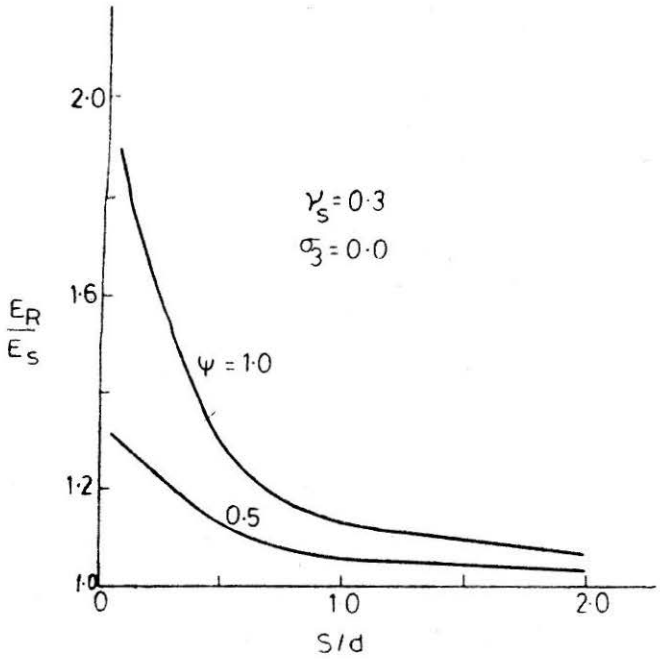

FIGURE 6 Equivalent Modular Ratio Versus Spacing

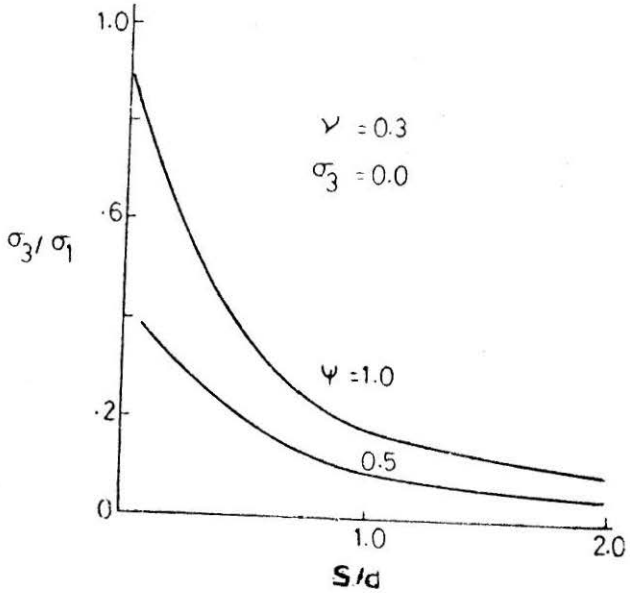

FIGURE 7 Equivalent Confining Stress Versus Spacing

The equivalent modulus of deformation of reinforced soil obtained from the present analysis is compared with experimental results of Broms (1988) and Rao *et al* (1987) in Table 1. The modulus values are normalised with those for a standard triaxial specimen (S/d or $H/R = 2.0$). The modular ratio (E_R/E_s) increases with the number of reinforcing layers, *i.e.* with decreasing ratio of S/d. Predictions are made with smooth $\Psi = 0$, and rough ends $\Psi = 1$, for the standard triaxial specimen. The predicted values of modular ratios are greater than 1.0 and increase with decreasing spacing, but smaller than the experimentally observed values. The present analysis predicts only the improvement in elastic modulus due to the restaining shear stresses on the two end surfaces but not the effect of equivalent confining stress on improving the modulus. Rao *et al* (1987) demonstrate the significant effect of confining stress on unreinforced and reinforced soil specimens. In their tests, the modulus increases from about 45 KPa at confining stress of 10.0 KPa to about 200 KPa at $\sigma_3 = 100$ KPa for the unreinforced soil. Increases of similar order are noticed even for reinforced soil. If the effect of the equivalent confining stresses are compounded to the elastic effects, the predicted modular ratios increase further and could fall in the same range as those measured. Thus the present work can be used to predict the equivalent modulus of deformation of reinforced soil considering both the restraining effects of shear stresses and of the equivalent confining stress.

TABLE 1

Comparison of Measured and Predicted Ratios of E_R/E_S

	No. of Reinf. Layers				
	0	1	2	3	Remarks
	S/d				
	2.0	1.0	0.667	0.5	
(i)	1.0	1.4	1.667	2.32	Fig. 6 Broms (1988) d = 100mm, σ_3 = 50 KPa
(ii)	1.0	1.24	—	1.53	Fig. 8 Broms (1988) d = 200mm, σ_3 = 50 KPa
(iii)	1.0	1.28	1.4	—	Rao *et al* (1987) Initial Tangent Modulus
(iv)	1.0	1.12	1.20	1.285	Predicted : Smooth ends, $\Psi = 0$
(v)	1.0	1.06	1.13	1.21	Predicted : Rough ends, $\Psi = 1$.

Conclusions

Balla's (1960) solution for the analysis of cylindrical specimen under triaxial stress conditions, is used to obtain axial and radial deformations. The axial displacement-influence coefficient, I_w, is shown to vary significantly with the spacing between the reinforcing layers, the Poisson's ratio of the soil, and the confining stress. The displacement profiles for samples with different spacing to diameter ratio also are presented. The equivalent modulus of deformation of and the equivalent confining stress on the reinforced soil are computed and given as functions of the spacing ratio. The measured and computed values of moduli of deformation compare well if both the effects of (*i*) the restraining action of the shear stresses on the top and bottom faces, and (*ii*) the equivalent confining stress are considered.

Acknowledgement

The computational help of Dr. J.S.V.R. Prasad, the neat and prompt typing of Sri U.S. Misra are gratefully acknowledged. The critical comments of the reviewer(s) are appreciated.

References

BALLA, A., (1960), "Stress Conditions in Triaxial Compression", *J. Soil Mech. and Foundn. Div.*, ASCE, Vol. 86, No. SM6, pp. 57-84.

BROMS, B.B. (1987), "Fabric Reinforced Soil", *The Post Vienna Con,. on Geotextiles*, Singapore, pp. 104-156

GRAY, D.H. and OHASHI, H., (1983), "Mechanics of Fibre Reinforcement in Sand", *J. Geotech. Engg. Div.*, ASCE, Vol. 109, No. GE3, pp. 335-353.

INGOLD, T.S. and MILLER, K.G. (1982), "Analytical and Laboratory Investigations of Reinforced Clay", *Proc. II Int. Conf. on Geotextiles,* Las Vegas, Vol. III, pp. 587-592.

McGOWN, A., ANDRAWES, K.Z. and Al-HASANI, M.M., (1978), "Effect of Inclusion Properties on the Behaviour of Sand", *Geotechnique*, Vol. 28, No. 3, pp. 327-346.

RAO, G.V., GUPTA, K.K. and KACHHAWAH, R. (1987), "Triaxial Behaviour of Geotextile Reinforced Sand", IGC-87 on Soil Properties, Problems and Practices, Bangalore, Vol. 1, pp. 323-328.

SCHLOSSER, F. and LONG, N.T., (1972), "Compartment de la Terre Armee' dans les Ouvrages de Soutenement", Proc. 5th ECSMFE, Madrid, Vol. 1, No. IIIa-a, pp. 299-306.

YANG, Z., (1972), "Shear Strength and Deformation Characteristics of Reinforced Sand", Doctoral Thesis, Univ. of Calif, Los Angeles

APPENDIX I

$$I_1 = z/H - \psi\varphi_w\nu/(1-\nu) \tag{A.1}$$

$$I_2 = -2\nu\, z/H + \psi\varphi_w (1-\nu) \tag{A.2}$$

$$I_3 = = -\nu\, r/R + \psi\varphi_u\nu/(1-\nu), \tag{A.3}$$

$$I_4 = (1-\nu)\, r/R + \psi.\phi_u \tag{A.4}$$

$$\varphi_w = Q\,[-3\nu(z/H) - 4\,(1-\nu)\,(H/R)^2\,(z/H) + 4\,(H/R)^2\,(z/H)^3 - T\,F\sigma_w] \tag{A.5}$$

$$\varphi_u = Q[-\frac{3}{2}(3-5\nu)\,\frac{r}{R} + 4(1-\nu^2)\,(H/R)^2\,(r/R) - 12(1-\nu^2)\,(H/R)^2\,(z/H)^2 \cdot (r/R) - \frac{3}{2}\,(1-\nu-2\nu^2)\,(r/R)^3 - T(1+\nu)\,H/R\,F\sigma_u] \tag{A.6}$$

$$F\sigma_w = \sum_{n=1}^{\infty} \frac{P}{n}\,[(1 - U_n\, 4(1-\nu)\,\frac{H}{n\pi R}\,J_{oR} - U_n J_{1r}]\quad \frac{\sin n\pi z}{H} \tag{A.7}$$

$$F\sigma_u = \sum_{n=1}^{\infty} \frac{P}{n}\,[U_n\,(r/R)\,J_{or} - J_{1r}]\cos\frac{n\pi z}{H} \tag{A.8}$$

$$T = \frac{24(1-\nu)}{\pi^2}\cdot\frac{H}{R} \tag{A.9}$$

$$P = \frac{\cos n\pi}{n\ V_n}\cdot\frac{1}{J_{1R}} \tag{A.10}$$

$$Q = 1/[3(1-\nu) + 8(1+\nu)\,(1 - 3\ K/\pi^2)\,(H/R)^2] \tag{A.11}$$

$$U_n = \frac{(3-\nu)\ \frac{1}{n\pi}\ H/R - (1-\nu)\ J_{oR}/J_{1R}}{\{(1-\nu)\ [4\ \frac{1}{(n\pi)^2}(H/R)^2 - 1] + (1+3\nu-2\nu^2)\ \frac{1}{n\pi}\ R/H\ \frac{J_{oR}}{J_{1R}}\}} \tag{A.12}$$

$$V_n = 1 - U_n\ [2(1-\nu)\ \frac{1}{n\pi^2}\ H/R + \frac{J_{oR}}{J_{1R}}] \tag{A.13}$$

$$K = \sum_{n=1}^{\infty} \frac{1}{n^2 V_n}\,[1 - U_n\, J_{oR}/J_{1R}] \tag{A.14}$$

$$J_{oR} = J_o\,(\text{in}\ \pi\ R/H) \tag{A.15}$$

$$J_{1R} = J_1\,(\text{in}\ \pi\ R/H)/i \tag{A.16}$$

$$J_{oR} = J_o\,(\text{in}\ \pi\ r/H) \tag{A.17}$$

$$J_{1r} = J_1\,(\text{in}\ \pi\ r/H)i \tag{A.18}$$

r and z the coordinates of point where w_s and u_s are evaluated, J_o and J_1 — Bessel functions of zero and first order respectively with imaginary arguments.

Notation

d — diameter of specimen

E_R — modulus of deformation of reinforced soil

E_S — modulus of deformation of soil

H — S/z—distance from centre of specimen to reinforcement layer

h — height of specimen

I_1—I_4 — influence coefficients

I_r — radial displacement coefficient

I_w — axial displacement coefficient

J_o, J_1 — Bessel functions of zero and first order

R — radius of specimen

r — radial distance

s — spacing between reinforcement layers

z — axial distance

ν_s — Poisson's ratio of soil

1′ 3 — axial and lateral stresses

Ψ — a measure of frictional resistance between reinforcement and the soil.